Pergamon

0301-9322(93)E0031-Y

Int. J. Multiphase Flow Vol. 20, No. 2, pp. 363–381, 1994

0301-9322/94 $7.00 + 0.00

PREDICTION OF DROP SIZE DISTRIBUTIONS IN SPRAYS USING THE MAXIMUM ENTROPY FORMALISM: THE EFFECT OF SATELLITE FORMATION

C. W. M. VAN DER GELD and H. VERMEER

Faculty of Mechanical Engineering, Eindhoven University of Technology, P.O. Box 513, 5600 MB Eindhoven, The Netherlands

(Received 25 June 1991; in revised form 1 June 1993)

Abstract—The droplet size distribution function for sprays is derived using the maximum entropy formalism (MEF) to link the end stage of the atomization process to an intermediate state, characterized by unstable liquid cylinders. The probability density function, PDF, for droplet diameter, δ, is mainly governed by conservation of mass and the energy equation. Many of the small droplets are supposedly created together with a much larger droplet, i.e. are supposed to be satellites. A dual PDF, $f_1(\delta, \delta^*)$, represents the number of satellites of diameter δ corresponding to a central or primary drop with diameter δ^*. The representation space is extended with the primary droplet diameter δ^* and the MEF is applied to derive the function f_1. The physical constraints are first related to parts of the liquid cylinders only, and some higher moments of the primary size distribution function, $f_0(\delta^*)$, have to be known in order to be able to apply the MEF. Some problems inherent in the application of this formalism are examined. Without invoking fitting parameters or *ad-hoc* constraints the predicted PDFs are close to measured ones.

Key Words: sprays, drop size, maximum entropy, distribution, satellite

INTRODUCTION

In this study the break-up of a liquid sheet into droplets is studied with the aid of the maximum entropy formalism (MEF). The MEF can be seen as an economic way to fulfil specific physical constraints to a process. It is not a substitute for the deterministic laws that help us to predict, for example, particle trajectories. It provides us with probabilities of the equilibrium particle settling velocities and positions. This is very similar to the traditional treatment of the extremal properties of thermodynamic potentials. It would not be appropriate to declare that the MEF is the clue to many difficult two-phase flow problems. But it would be equally inappropriate not to investigate the possiblities of this formalism, especially in the realm of distribution phenomena in two-phase flows where a variational approach to entropy production has been found to work properly for some specific cases (van der Geld 1985; van der Geld & Nijdam 1991).

The MEF generally links two stages of a process; let, for ease of reference, these stages be denoted as A and B. Just as in the variational approach of classical mechanics there is no *a priori* justification for the choice of, for example, the Hamiltonian, there is no *a priori* justification for the choice of constraints in the MEF. If, however, external conditions leading to stage A are such that a certain wavelength dominates, the formalism should be provided with this information, either through the governing equations or otherwise. If some details of the break-up process influence stage B, then the formalism should be provided with information concerning these details. If, for example, surface contraction and liquid extraction in an intricate manner combine to produce satellites, the formalism must be allowed to accomodate satellites.

Many authors have contributed to the knowledge of the formation of droplet sprays (e.g. Lefebvre 1983). Many practical correlations exist for the droplet size probability density function (PDF) but the best ones seem to suffer from a lack of theoretical foundation, see Bhatia & Durst (1989). Most of the theoretical studies do not yield any description of the spray beyond some expression for an average or maximum drop diameter on the basis of the most readily amplified disturbances.

The works of Dombrowski & Johns (1963), Sellens (1987) and Li & Tankin (1988) are of particular interest in the present work. The first authors split up the spray formation process into different, successive stages and their description of the first stage is adopted here. Sellens (1987) seems to have been the first to try the MEF, using basic conservation principles to predict drop size distributions. He added momentum and kinetic energy constraints to derive joint distributions of drop size and velocity. He also added an *ad-hoc* constraint which he called "partition of surface energy". This partition constraint was needed to reduce the number of small droplets in the PDF that had been obtained by merely using the conservation equations. An unknown parameter of the partition constraint was used to fit the predicted PDF to the extensive set of accurately measured distribution functions. The predictions of the present study will be compared to these data.

Li & Tankin (1988) more or less modified the Sellens approach, but unfortunately made the same mistake as did Jaynes (1983) in the early days of developing the entropy formalism. This will be explained in this paper.

In this study, an attempt is made to demonstrate that the MEF is suitable for predicting realistic droplet size distribution functions for sprays. Since considerable experimental evidence exist for the occurrence of satellites, an effort is made to account for this complicated mechanism. This is done with the aid of a composite, quasi-multidimensional distribution function. *Ad-hoc* postulates are not introduced and no parameters are fitted to the experimental data. The number of constraints is kept as low as possible to maintain the clarity of the approach and the traceability of the physics and to emphasize that the MEF is in essence simple and straightforward.

The physical picture underlying the model is thoroughly discussed. The applicability of the MEF is examined and the results are compared with experimental findings and results obtained by other authors.

Outline of the approach

This paper presents a formalism for calculating spray structures using:

(1) A physical model for liquid sheet break-up.
(2) A probability density function, f, for droplet sizes.
(3) Overall mass and energy conservation.
(4) Maximization of an entropy based on f subject to conservation constraints.

It appears that previous studies used the latter three and required additional constraints to reach agreement with observations. This study specifies initial and final states in terms of ligaments and droplets, reducing the parameter space to be studied by adapting the function f for the occurrence of satellites and by confining constraints to "units", parts of ligaments. With the constraints, and remaining free parameters within ranges that are in agreement with experiments and produce legal PDFs, realistic functions result.

THE PHYSICAL MODEL

In this section the process of liquid sheet disintegration is examined. Satellite formation is discussed and then the basic set of equations are derived.

The break-up of a liquid sheet

A viscous liquid sheet in quiescent, inviscid, gaseous surroundings breaks up into cylindrical liquid rolls, ligaments, due to growing sinusoidal disturbances, as shown in figure 1. Surface tension, aerodynamic and liquid viscous forces govern this process (Lefebvre 1983; Ohnesorge 1936; Dombrowski & Johns 1963).

In the model of Dombrowski & Johns (1963) a value for ligament diameter, $d_{\text{lig}}^{\text{theo}}$, is computed. This value depends on the thinning rate:

$$d_{\text{lig}}^{\text{theo}} = 0.84\delta_{30}^{\text{exp}}. \qquad [1]$$

Here δ_{30}^{exp} denotes an experimentally-determined mass mean diameter (MMD) and is not dimensionless. Although the computation is not particularly simple, the predicted value is close to reality according to the direct measurements of Sellens (1987):

$$d_{lig\,exp} = (0.87 \pm 0.07) \cdot \delta_{30}^{exp}, \quad [2]$$

with 0.07 being the standard deviation of 6 measurement data. Different experiments determined the value of the mass mean diameter in [1] and [2].

The Dombrowski & Johns (1963) model has proven its validity and is now well-accepted (e.g. Theissing 1976). Their model describes disintegration into ligaments, whereas our model more particularly links the ligament stage with the droplet cloud.

A typical value of the ligament diameter, d_{lig}, for air–water systems is 80 μm according to Sellens (1987). Ligament diameter d_{lig}^{theo} is adopted as a given input parameter for our model. In general, it depends on the nozzle geometry and upstream conditions. In the governing equations it will appear in some constraints, e.g. c_1 and c_2.

The break-up of ligaments

Each ligament, roughly a liquid cylinder or thread, suffers from disintegration by air action or liquid turbulence, as illustrated in figures 1 and 2. The ligament falls apart due to the physical mechanisms explained by Weber (1931) and Rayleigh (1878), with the most dominant wavelength, L, given by

$$L = 4.5 d_{lig}. \quad [3]$$

This relation will be used in the mass and energy conservation equations. Our model is not based on deterministic or instability equations to actually compute the formation of droplets from ligaments but follows a different route, the MEF.

Since L is approximately uniform along the ligament, a "unit cell" can be defined as the part of the liquid cylinder with length L that encompasses a primary droplet kernel and two halves of the liquid bridging between droplet kernels (see figure 1). Dombrowski & Johns (1963) have also computed the MMD, δ_{30}, but this value is predicted much less accurately than the wavelength L and the distance of ligament disintegration to the nozzle outlet. In their model each unit cell evolves into one single droplet with diameter $\delta_{30\,theo}$. This yields values that systematically differ from experimental results (Dombrowski & Johns 1963; Sellens 1987; Theissing 1976):

$$\delta_{30}^{exp} = F\delta_{30\,theo} \quad \text{with} \quad 0.58 < F < 0.68. \quad [4]$$

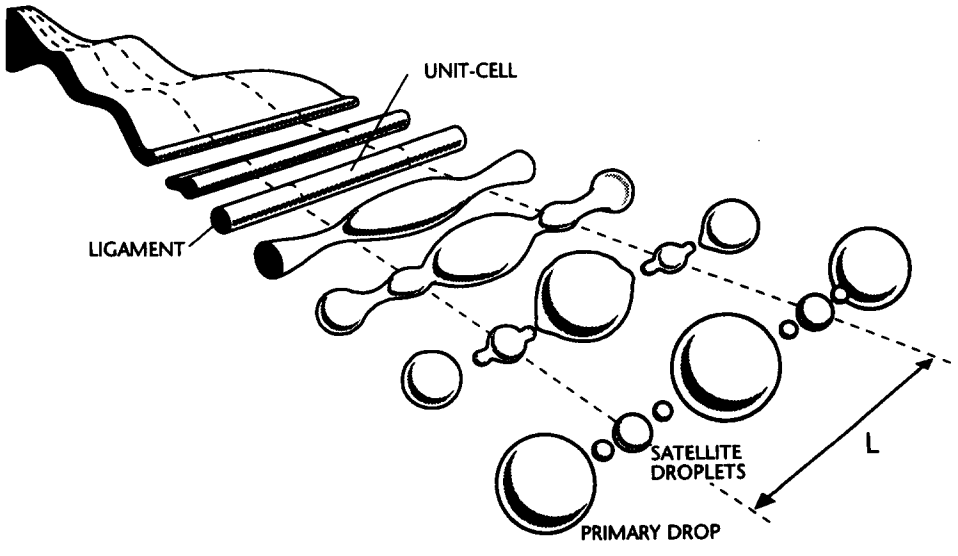

Figure 1. Idealized disintegration of a liquid sheet into ligaments, after Dombrowski & Johns (1963), and idealized disintegration of ligaments into droplets.

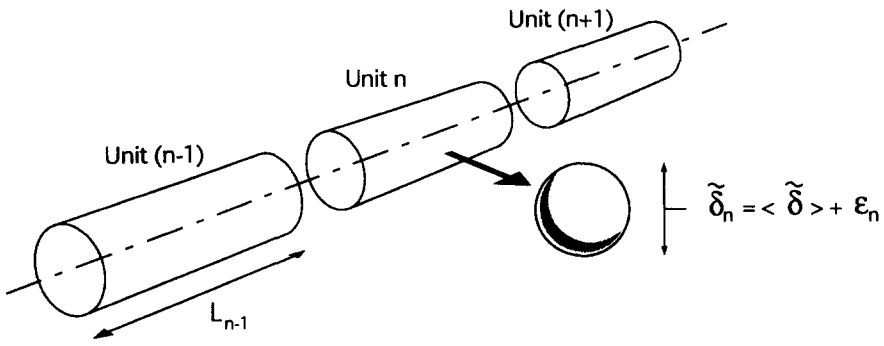

Figure 2. Definition of spread of the mass equivalent diameter, $\tilde{\delta}$.

For ease of reference a mass equivalent diameter, $\tilde{\delta}$, is defined by

$$\pi d_{\text{lig}}^2 L/4 = \pi\tilde{\delta}^3/6 \rightarrow \tilde{\delta}^3 = 1.5 d_{\text{lig}}^2 L. \qquad [5]$$

See figures 2 and 3. Combining [3] and [5], and putting $\delta_{30\,\text{theo}} = \tilde{\delta}$, Dombrowski & Johns (1963) obtained

$$\delta_{30\,\text{theo}} = 1.88 d_{\text{lig}}, \qquad [6]$$

which yields [2] after using [4] to correct for the experimental findings.

However, the amount of surface energy that would have to be liberated during the unit disintegration is now easily computed to be ca. 21% of the originally available surface energy, $\pi\sigma d_{\text{lig}} L$; σ is surface tension. Since all this energy would have to be dissipated by internal droplet movements, it is more likely that some part of the excess surface energy is spent in the formation of satellite droplets. More arguments for the occurrence of satellite drops will be given in the following.

The formation of satellites

The discrepancies between the above theoretical and experimental values of δ_{30} are partly due to the occurrence of satellite droplets and partly due to oversimplifications in the deterministic theories that are not discussed here. We do not follow a mechanistic approach in which simplifications are bound to occur, but will rather compare two different quasi-stationary states of the fluid. The first is the ligament state and the second is the droplet cloud state.

The diameter that corresponds to the largest of all droplets that are formed in a unit cell is defined to be the primary drop parameter, δ^*. The other drops are called satellites and their diameter will be denoted by δ_s. The predicted value of the mass equivalent diameter, $\tilde{\delta}$, is adopted as an upper

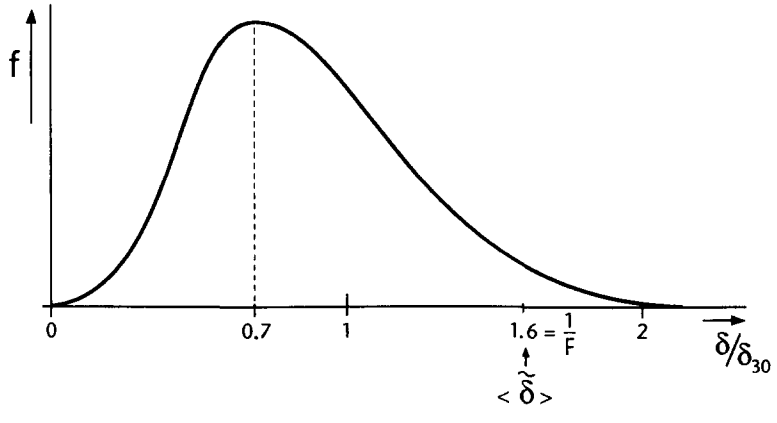

Figure 3. Schematic of the PDF, f, of the dimensionless droplet diameter, δ, and some approximated values.

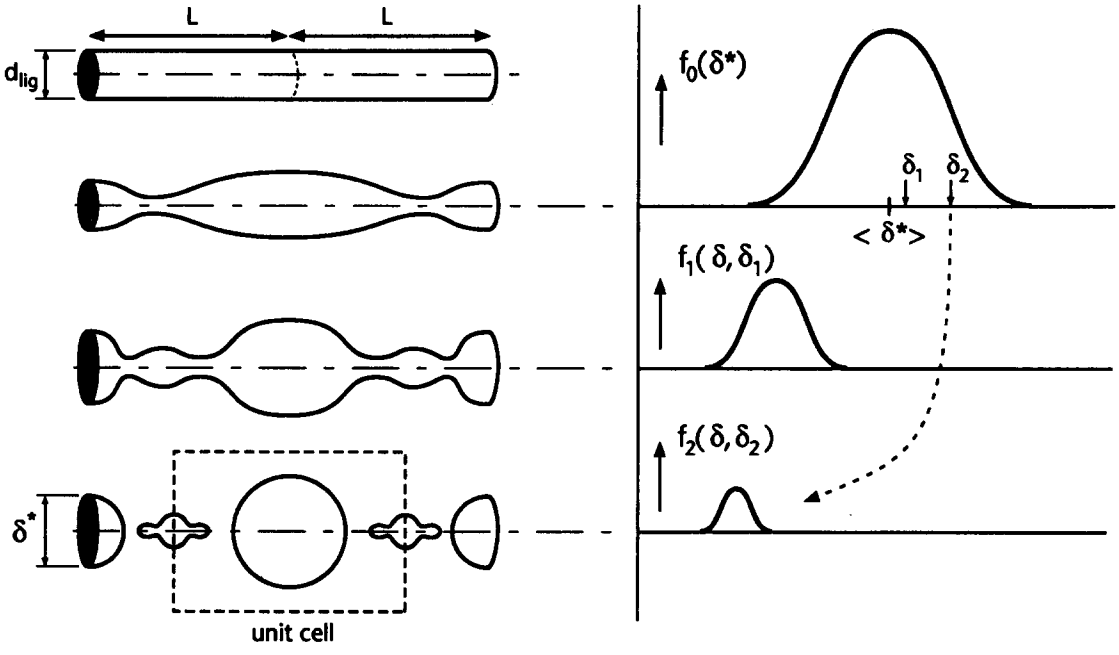

Figure 4. Schematic of unit cell disintegration and satellite distribution functions.

bound for δ^*. Because of [5] this upper bound depends on d_{lig}, but the range of values accessible to δ^* will be seen to be so large that the mean value of δ^* can be considered as an independent input parameter to our model. How this mean value is determined will be seen in the following.

Both δ^* and δ_s are made dimensionless by dividing by the δ_{30}^{exp}, which typically amounts to 100 μm.

Note that the discrimination between primary droplets and satellites is obvious in the process of ligament disintegration but would be arbitrary in a droplet cloud.

The liquid bridging connecting two droplet kernels in a ligament (see figures 1 and 4) appears to be unstable, which leads to the formation of satellites (Tebel 1982; Beer & Chigier 1972; Mansour & Lundgren 1990; Chesters 1990). The formation of satellites is a non-linear phenomenon occurring during a short time before break-off of primary drops. The primary droplet itself is stable since relative velocities are too small to distort the large fluid contraction, as indicated by too low a value for the Weber number, We. In the later stages of spray development, aerodynamic forces may affect large drops but here only the primary stages that lead to the formation of a droplet cloud are considered.

There is some indication (Mansour & Lundgren 1990; Chesters 1990) that the liquid bridgings between a satellite and its neighbours is also unstable. This might cause repetition of the process of liquid contraction in bridgings. The process stops as soon as the time of disintegration, t_0, exceeds the time of contraction into spheres. If $d_{lig} = 80\ \mu$m, an order-of-magnitude analysis for a viscous water column yields $t_0 \leqslant 1\ \mu$s, see Tebel (1982). If the same order of magnitude prevails in slightly viscous or non-viscous fluids, satellites are likely to occur since the emptying of relatively large liquid bridgings would take more time.

The exact point at which subsatellite formation stops is irrelevant in the present analysis.

The numerical analysis of Mansour & Lundgren (1990) shows that each unstable wavelength leads to satellite formation. Since, according to their results, all wavelengths exceeding πd_{lig} are unstable, satellite formation should be a common phenomenon.

Averaging over unit cells

There are several reasons why different unit cells have different values for the mass equivalent diameter, $\tilde{\delta}$.

To begin with, each instability phenomenon has a stochastic character. It requires triggering by some external agency. In most stability analyses such an excitation mechanism is just supposed to exist. However, in the absence of external triggering, the instability phenomenon for some part of a ligament may be strongly delayed. In that case, the value of $\tilde{\delta}$ will appear to be different for different unit cells, see figure 2.

Other reasons for dispersion of $\tilde{\delta}$ are the dispersion of wavelength and external causes influencing the growth rate.

The average value of $\tilde{\delta}$ is denoted by $\langle\tilde{\delta}\rangle$. Following Dombrowski & Johns (1963), we take $\langle\tilde{\delta}\rangle = \delta_{30}^{\exp}/F = 1,6\delta_{30}^{\exp}$, see [4] and figure 3.

Due to the spread in $\tilde{\delta}$ and the formation of satellites, the value of the primary drop diameter, δ^*, is spread around some mean value, $\langle\delta\rangle^*$. The probability of finding a primary droplet diameter in the range $[\delta^*, \delta^* + \mathrm{d}\delta^*)$ is denoted by $f_0(\delta^*)\,\mathrm{d}\delta^*$, with f_0 assumed to be Gaussian distributed:

$$f_0 = A\sqrt{k/\pi}\,\exp(-k\{\delta^* - \langle\delta^*\rangle\}^2). \qquad [7]$$

The PDF f_0 represents the chance of getting a primary drop when selecting a droplet out of all droplets that are formed out of a unit (an ensemble of units has to be considered to obtain a PDF). The value of A, therefore, only equals 1 if no satellites are formed. The variance is given by $1/(4k)$. The value of k is typically around 7.5–10 but is varied to examine its influence. Values for k exceeding 10 can only occur if very low values of the dimensionless amplitude A are acceptable. Amplitude A is introduced for normalization purposes and is further discussed in the following. It will be shown that very low values of A are unlikely whence the upper bound of k is reasonable. If $k < 7.5$, the chance of primary drops with a size of about d_{lig} becomes too large in view of the estimate of d_{lig} to come.

A typical value for $\langle\delta^*\rangle$ is 1.2 with an upper bound of 1.6, since $\langle\tilde{\delta}\rangle = 1.6 \cdot \delta_{30}^{\exp}$ as discussed above. It is easy to see that the MMD is less than the mass mean primary droplet diameter, hence $\langle\delta\rangle^*$ is always in the range [1.0; 1.6].

The PDF for finding a droplet with diameter δ in the droplet cloud after disintegration of the liquid sheet will be denoted by $f(\delta)$ (see figure 3). The aim of this study is the theoretical prediction of the distribution function with the aid of maximization of entropy.

A COMPOSITE DISTRIBUTION FUNCTION TO ACCOUNT FOR SATELLITE DROPS

Consider an ensemble of, say, 10^{10} ligaments. Let N denote a total number of droplets stemming from these ligaments. The number of primary droplets with diameters in the range $[\delta^*, \delta^* + \mathrm{d}\delta^*)$ is given by $N \cdot f_0(\delta^*) \cdot \mathrm{d}\delta^*$.

Let the number $\tilde{N}(\delta^*) \cdot f_1(\delta, \delta^*) \cdot \mathrm{d}\delta$ represent the number of satellites with diameter in the range $[\delta, \delta + \mathrm{d}\delta)$ for a drop δ^*. Here $\tilde{N}(\delta^*)$ denotes the total number of satellite droplets corresponding to "a drop δ^*" which is shorthand for "a primary droplet with diameter δ^*". In appendix A a derivation is given of the following expression for the PDF:

$$f(\delta) = f_0(\delta) + \int \tilde{N}(\delta^*) f_0(\delta^*) f_1(\delta, \delta^*)\,\mathrm{d}\delta^*. \qquad [8]$$

See figure 4. The total number of satellites with diameter in the interval $[\delta, \delta + \mathrm{d}\delta)$ is given by

$$\int N f_0(\delta^*) f_1(\delta, \delta^*)\,\mathrm{d}\delta^*\,\mathrm{d}\delta. \qquad [9]$$

The probability of finding a satellite with diameter δ in the range $[\delta, \delta + \mathrm{d}\delta)$ to a primary drop with diameter δ^* is either:

—zero (no satellites in the specified range formed with drop δ^*); or
—$f_1(\delta, \delta^*)\,\mathrm{d}\delta$.

In the latter case $\int f_1(\delta, \delta^*)\,d\delta = 1$, since we are sure to find a satellite of some diameter; in the first case the integral has no meaning. Since this is supposed to hold for an infinite number of drops δ^*, also an infinite number of normalization conditions exists, all of the form

$$\int f_1(\delta, \delta^*)\,d\delta = 1.$$

The way to handle this is described below.

Equating the total number of droplets, N, to the sum of totals already given for primary drops, $N\int f_0(\delta^*)\,d\delta^*$, and satellites, [9], and dividing by N yields the global normalization equation:

$$1 = \int f_0(\delta^*)\,d\delta^* + \iint f_0(\delta^*)\tilde{N}(\delta^*)f_1(\delta, \delta^*)\,d\delta^*\,d\delta. \qquad [10]$$

Since $\int f_0(\delta^*)\,d\delta^* = A$, A must be <1. In a manner that will be discussed shortly, the value of parameter A is made consistent with the choice of $\tilde{N}$ and [10].

The interpretation of A is as follows. In each unit there is, by definition, only one primary droplet. Division of [10] by A therefore shows that $1/A$ is the total number of drops in a unit and that $1/A - 1$ is the total number of satellites in the unit. Since the MMD is also the MMD of the droplets in a unit, conservation of mass yields:

$$\delta_{30}^3 = A \cdot \tfrac{3}{2} \cdot 4.5 \cdot d_{\text{lig}}^3 \rightarrow \delta_{30} = 1.89 d_{\text{lig}} A^{1/3}. \qquad [11]$$

The only free parameters in the model are therefore those describing the primary droplet distribution f_0 (k and $\langle\delta^*\rangle$), those describing the satellite number density $\tilde{N}$ (entailing 1 or 2 parameters that will soon be discussed) and d_{lig}. Our approach is phenemological in the sense that the parameters describing f_0, $\tilde{N}$ and d_{lig} can be adapted to the system parameters, e.g. the specific nozzle geometry.

Note that an experimental value for the number of satellites, $1/A - 1$, can be inferred from [11] and [2]. It yields about 3.4, which again indicates that in actual atomization processes satellites are bound to occur. A is typically in the range 0.2–0.5, corresponding to 1–4 satellites.

Although $\tilde{N}$ is not known *a priori*, this functional relationship must satisfy requirements that are strong enough to make the results relatively independent of the particular choice of $\tilde{N}$. To begin with, tiny droplets do not have satellites since they cannot be primary drops. There exists, therefore, a threshold, δ^*_{min}, with $\tilde{N}(\delta) = 0$ if $\delta < \delta^*_{\text{min}}$. Wavelengths less than d_{lig} are not expected to produce droplets (Mansour & Lundgren 1990). Therefore, δ^* must be substantially larger than d_{lig}, see figures 1 and 2. Most of the droplets with δ less than about d_{lig} must therefore be satellites. So the dimensionless ligament diameter $\bar{d}_{\text{lig}} \equiv d_{\text{lig}}/\delta_{30}$ is a reasonable estimate for δ^*_{min}. Furthermore, the $\tilde{N}$ should have discrete values and should be monotonously increasing with increasing primary droplet size. The latter can be seen as follows. The ratio L/d_{lig} is approximately constant because of [3]. A large δ^* value requires large a value d_{lig} (see figure 2). This corresponds to a large unit width, L, which requires long liquid bridgings and therefore many satellites.

In order to make $\tilde{N}$ amenable to numerical evaluation, it is approximated by a continuously differentiable function starting from 1 (see figure 5). If $\tilde{N}$ is polynomial expanded according to

$$\tilde{N}(\delta^*) = b_0 + b_1\delta^* + b_2\delta^{*2}, \qquad [12]$$

then b_0 is fixed by $\tilde{N}(\delta^*_{\text{min}}) = 1$. The best results are obtained with rather rapidly increasing functions, which is easily understood from the fact that $\tilde{N}$ should be an increasing function with discrete values.

Now [10] can be reduced with the aid of the normalization of f_1. Since

$$\iint f_0(\delta^*)\tilde{N}(\delta^*)f_1(\delta, \delta^*)\,d\delta^*\,d\delta = \int \left\{\int f_1(\delta, \delta^*)\,d\delta\right\} f_0(\delta^*)\tilde{N}(\delta^*)\,d\delta^* = \int f_0(\delta^*)\tilde{N}(\delta^*)\,d\delta^*,$$

this yields

$$1 = \int \{1 + \tilde{N}(\delta^*)\} f_0(\delta^*)\,d\delta^*,$$

which in combination with [12] yields integrals that are solved analytically. The result is

$$1 = (1 + b_0)A - b_1\langle\delta^*\rangle A + b_2 A(1/2k + \langle\delta^*\rangle^2). \quad [13]$$

This equation connects the amplitude A with the satellite number density $\tilde{N}$.

GOVERNING EQUATIONS

The transition from ligaments into droplets requires a short period of time and is governed by capillary forces, see above, and we therefore consider conservation of surface energy to be the most important governing law. The actual surface energy in a unit in [J] is given by the sum of the satellite surface energy and that of the primary droplets:

$$\pi\sigma \int \delta^2 \delta_{30}^2 \tilde{N}(\delta^*) f_1(\delta, \delta^*)\, \mathrm{d}\delta + \pi\sigma\delta^{*2}\delta_{30}^2. \quad [14]$$

The break-up process in essence encompasses the perpetual and multiple disintegration of unit cells. The set of basic equations for each unit cell is given by [15]:

normalization,

$$\int f_1(\delta, \delta^*)\, \mathrm{d}\delta = 1; \quad [15a]$$

conservation of surface energy,

$$\int \delta^2 \tilde{N}(\delta^*) f_1(\delta, \delta^*)\, \mathrm{d}\delta = c_1 - \delta^{*2} - S_{\mathrm{diss}}; \quad [15b]$$

and

conservation of mass,

$$\int \delta^3 \tilde{N}(\delta^*) f_1(\delta, \delta^*)\, \mathrm{d}\delta = c_2 - \delta^{*3}. \quad [15c]$$

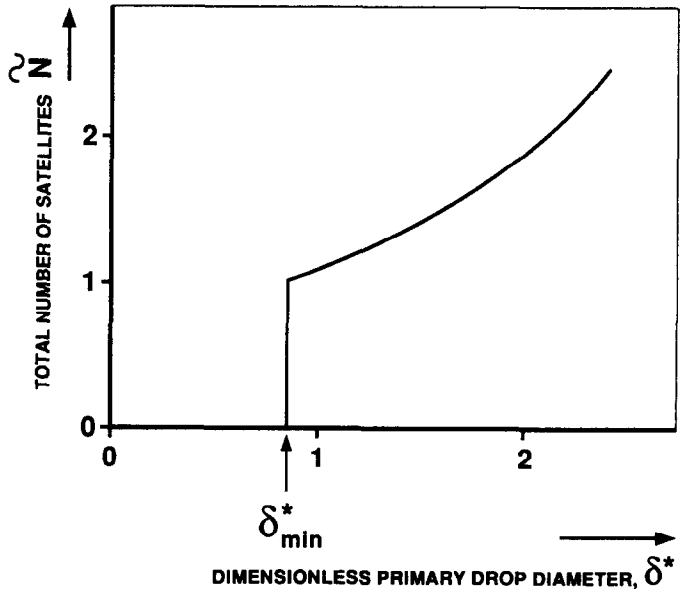

Figure 5. Specimen of the relationship between the number of satellites, $\tilde{N}$, and the primary drop diameter, δ.

Expressions [15a–c] hold for each primary droplet with diameter δ^* having at least one satellite. The dissipated energy is accounted for by S_{diss}, either known or estimated. In this study S_{diss} is put equal to zero without loss of generality. By neglecting energy dissipation we merely concentrate on the many practical break-up regimes in which surface tension forces are much larger than viscous forces and liquid inertial forces are small, see Ohnesorge (1936).

The constant $c_1 = d_{\text{lig}} L/\delta_{30}^2 = \bar{d}_{\text{lig}} L/\delta_{30}$, which typically amounts to 3.45–3.8 (using [3] and [2] $4.5 \cdot d_{\text{lig}}^2/\delta_{30}^2 \approx 4.5 \cdot 0.87^2$). The constant $c_2 = 1.5(\bar{d}_{\text{lig}})^2 L/\delta_{30}$ and is typically 4.6–4.9 (again using [2] and [3]).

Equations [15a–c] could, in principle, be extended with the conservation of linear impulse in the streamwise and transversal directions and with conservation of kinetic energy. However, the physical information contained in [15a-c] will suffice for the prediction of realistic PDFs.

THE MAXIMUM ENTROPY FORMALISM (MEF)

The MEF provides us with a best estimate of a PDF when a system goes from one-quasi-stationary state to another, based on some given information (Jaynes 1983). Nowadays, the MEF is recognized as a generally applicable method of statistical inference.

Let g_i denote a general type of state function of a physical system and $\langle g_i \rangle$ its expectation value that is presumably known as a bulk property of the physical system. The solution space is described by the differential form $\mathrm{d}\Omega$, e.g. equal to $\mathrm{d}\delta \cdot \mathrm{d}u \cdot \mathrm{d}v$. Let all knowledge of the physical system be expressed in n constraints, all of the form

$$\int f g_i \, \mathrm{d}\Omega = \langle g_i \rangle, \qquad [16]$$

with f denoting the PDF that is normalized to 1. In the MEF the least-biased distribution is determined by maximization of an entropy that was first formulated in terms of a discrete set of parameters. Jaynes (1983) derived the continuous entropy

$$S_{\text{cont}} = -k \int f(x) \ln[f(x)/m(x)] \, \mathrm{d}x, \qquad [17]$$

with m denoting a measure of the solution space that is 1 in our case (standard Borel–Lebesgue measure). The general form of the measure will be needed in the discussion of Li & Tankin's paper (1988). This measure assures that the entropy is invariant under transformations. It also ensures that the formalism is in agreement with Jaynes consistency principle that reads "Two problems with the same relevant physical information show the same PDF's".

By maximizing the entropy of [17] the distribution function is found to be

$$f = \exp(-\lambda_0 - \lambda_1 g_1 - \lambda_2 g_2 - \cdots - \lambda_n g_n), \qquad [18]$$

where the λ_i denote as-yet undetermined Lagrange multipliers. The multiplier λ_0 takes account of normalization. If all multipliers are known the PDF, f, is determined. However, the implementation of the MEF is not an easy task, as is illustrated in figure 6. It depicts what may happen if incorrect averages are used and convergence is not really achieved. Figure 6 is discussed more fully in appendix B, where numerical details are presented.

RESULTING PDFs WITH CONSTRAINTS AND A REVIEW OF RELATED RESEARCH

Resulting PDFs

The regular solution of [15a–c] would read $\exp\{-\lambda_0'(\delta^*) - \lambda_1'(\delta^*) \cdot \delta^2 - \lambda_2'(\delta^*) \cdot \delta^3\}$ according to the MEF as shown above. This expression is far too difficult to handle, since the dependencies of the functions λ_i on δ^* are unknown.

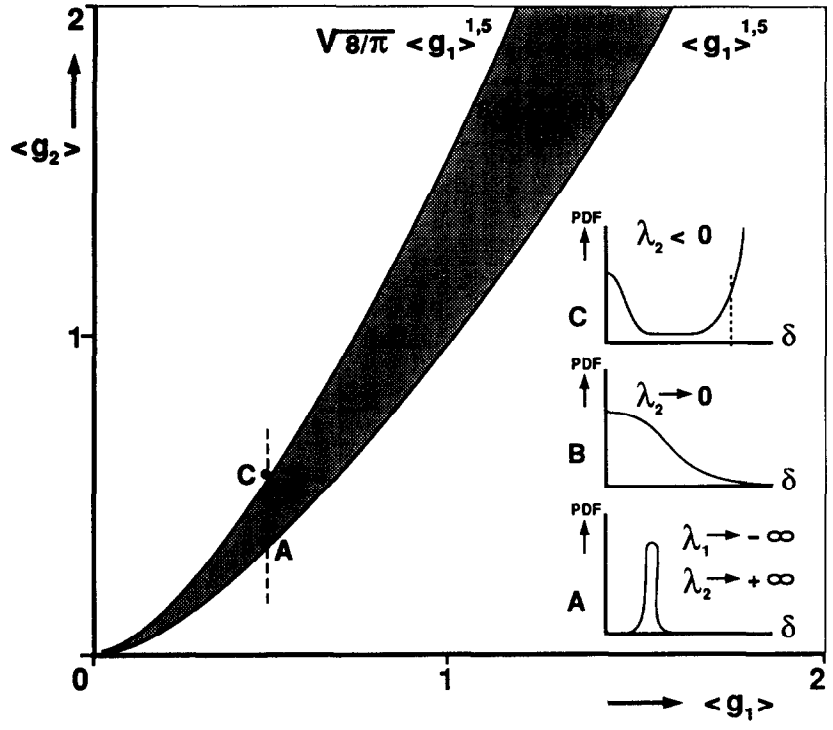

Figure 6. Solution space and typical examples of PDFs for only two physical constraints (zero-order moment only).

In appendix C it is shown how [15a–c] are made more accessible, taking full advantage of the fact that the primary size distribution function is relatively well-known. The resulting PDF is denoted as $\tilde{f}$ and with the aid of the MEF is solved to be

$$\tilde{f} = \exp[-\lambda_0 \quad -\lambda_1\delta^2 - \lambda_2\delta^3 + -\lambda_3(\delta^* - \langle\delta\rangle^*) - \lambda_4\delta^2(\delta^* - \langle\delta\rangle^*)$$
$$-\lambda_5\delta^3(\delta^* - \langle\delta\rangle^*) + -\lambda_6(\delta^* - \langle\delta\rangle^*)^2 - \lambda_7\delta^2(\delta^* - \langle\delta\rangle^*)^2$$
$$-\lambda_8\delta^3(\delta^* - \langle\delta\rangle^*)^2 + \cdots]. \qquad [C4]$$

It is noted that an alternative way to look at [C4] is by considering it as resulting from a polynomial expansion of the $\lambda_i'(\delta^*)$ functions that came into the solution of [15a–c].

In appendix D it is shown that $\lambda_3, \lambda_9, \lambda_{15}, \ldots$ can be well-approximated by zero. By taking $\lambda_6 = k$ and $\lambda_{12} = \lambda_{18} = \cdots 0$, the solution for $\tilde{f}$ is then demonstrated to be equal to $f_0(\delta^*) \cdot f_1(\delta, \delta^*)$. This allows us to skip all higher-order normalization constraints. The resulting set of equations reads:

$$\iint f_0 f_1 \, d\delta \, d\delta^* = A \iint \delta^2 \tilde{N} f_0 f_1 \, d\delta \, d\delta^* = c_1^0 \iint \delta^3 \tilde{N} f_0 f_1 \, d\delta \, d\delta^* = c_2^0, \qquad [19]$$

$$\iint (\delta^* - \langle\delta\rangle^*)\delta^2 \tilde{N} f_0 f_1 \, d\delta \, d\delta^* = c_1^1 \iint (\delta^* - \langle\delta\rangle^*)\delta^3 \tilde{N} f_0 f_1 \, d\delta \, d\delta^* = c_2^1, \qquad [20]$$

and

$$\iint (\delta^* - \langle\delta\rangle^*)^2\delta^2 \tilde{N} f_0 f_1 \, d\delta \, d\delta^* = c_1^2 \iint (\delta^* - \langle\delta\rangle^*)^2\delta^3 \tilde{N} f_0 f_1 \, d\delta \, d\delta^* = c_2^2, \qquad [21]$$

with the solution, according to the MEF,

$$f_1 = \exp[-\lambda_0 - \lambda_1\delta^2 - \lambda_2\delta^3 - \lambda_3\delta^2(\delta^* - \langle\delta\rangle^*) - \lambda_4\delta^3(\delta^* - \langle\delta\rangle^*) - \lambda_5\delta^2(\delta^* - \langle\delta\rangle^*)^2 - \lambda_6\delta^3(\delta^* - \langle\delta\rangle^*)^2] \quad [22]$$

with the Lagrange multipliers, λ_i, determined in the manner described in appendix B.

The set [22] was found to be robust in the sense that, in applying the MEF, convergence is almost always readily achieved.

Critical inspection of previous models

The primary problem of Sellens (1987) original approach was that his probability distribution was too high for very small droplet size. Li & Tankin (1988) tried to solve the problem by considering the droplet volume rather than the droplet diameter. However, without introducing a proper measure, m, the Shannon entropy of [17] is not an invariant. Li & Tankin did not take this measure into account, which lead to erroneous results.

Sellens & Brzutowski (1986; Sellens 1987) tried to reduce the number of small droplets by invoking a "partition constraint" $\iiint f/\delta \, d\Omega = K_p$ that fixes the mean surface-to-volume ratio. The value of K_p was determined by varying K_p until the theoretical PDF corresponded to the experimental one. In our view, data fitting according to $\Sigma_i 1/\delta_i = K_p$ was within Sellens' reach and would have been more appropriate. Here $\{\delta_i\}_i$ is the set of measured diameters; δ_i might be equal to δ_j for $i \neq j$. The "partition constraint" merely served as a tuning parameter. In addition, we consider the fixing of K_p as an *ad-hoc* postulate without much bearing to the actual physics involved. It, therefore, does not appear in the model presented in this paper.

We also find it less justifiable to introduce a second tuning parameter. Sellens also adjusted the mean surface energy, whereas a theoretical estimate of ligament thickness would have been possible since a Dombrowski & Johns (1963) type model had already been exploited to derive liquid film parameters. Moreover, Sellens selection of partly tuned, partly correlated average values leads to solutions of type C in figure 6, as demonstrated by figures 7 and 8. Sellens did not use the algorithm of Alhassid *et al.* (1978).

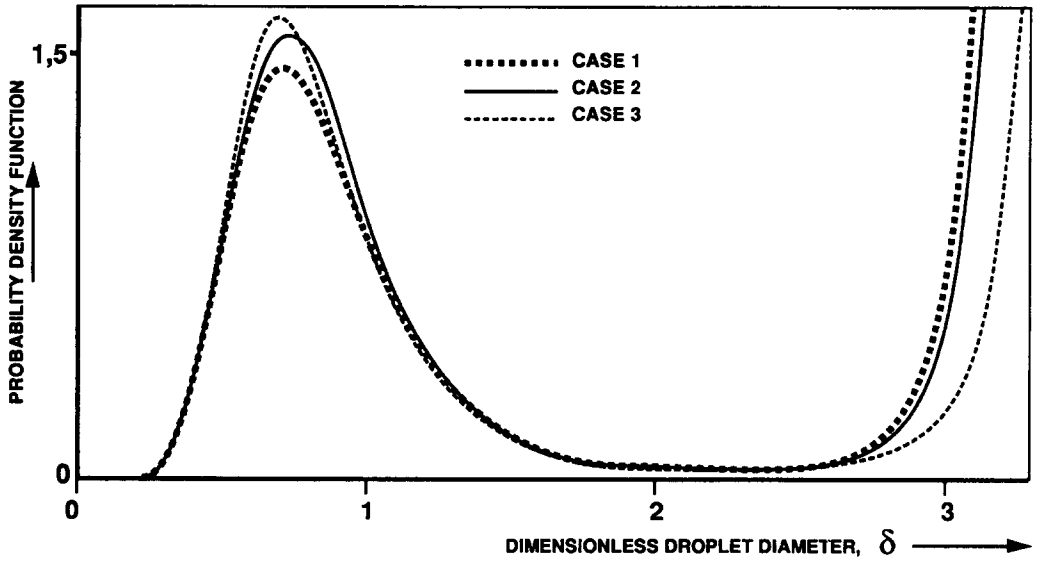

Figure 7. The effect of the integration boundaries in the velocity space on the size of the PDF. Averages are adopted from Sellens (1987): $\langle u\rangle = 1.0110397$; $\langle v\rangle = 0$; $\langle$mass$\rangle = 1$; $\langle$kinetic energy$\rangle = 1.1137712$; $\delta_{30}/\delta_{32} = 0.827$; $K_p = 1.4$. Velocity boundaries are taken as follows: case 1—$\langle u\rangle \pm 0.4$, $\langle v\rangle \pm 0.4$; case 2—$\langle u\rangle \pm 0.6$, $\langle v\rangle \pm 0.6$ (Sellens' choice); case 3—$\langle u\rangle \pm 0.8$, $\langle v\rangle \pm 0.8$.

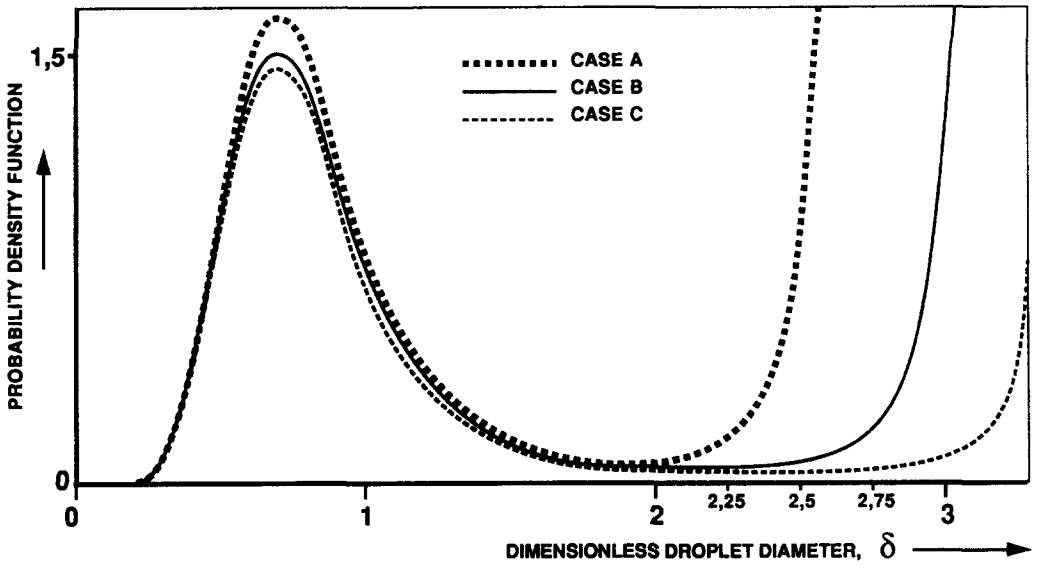

Figure 8. The effect of integration boundaries of the droplet diameter on the size of the PDF. Averages are adopted from Sellens (1987) (see figure 7). Dimensionless diameter boundaries are 0.05 and those indicated in the figure: case A—2.25; case B—2.50 (Sellens' choice); case C—2.75.

It should be well-noted that the above criticism is not meant to distract from the importance of Sellen's work. To our knowledge he was the first to use the MEF to predict droplet size distributions.

Figures 7 and 8 exhibit the importance of the integration boundaries for accurate numerical PDF prediction. Note that the normalization in figure 7 is satisfied, since the velocity dimensions are not shown. The problem is that apparently good convergence is reached, whereas actually the mean values may not properly be balanced, as noted above. Both Sellens (1987) and Li & Tankin (1988) have proclaimed that integration boundaries would not be important provided the physical variations were covered. This is incorrect. Expanding the error-function for small boundaries and small droplet diameter the PDF is easily seen to be proportional to the velocity range.

The integration boundaries in the present study typically are 0.00001 and 3.5 for δ and $d_{\text{lig and}}$ 3.5 for δ^*. Note that all governing equations except the normalization constraint contain $\tilde{N}(\delta^*)$, which is zero for $\delta^* < d_{\text{lig}}$; the normalization equation only applies to primary droplets that do have satellites.

Comparison with the present study

The conservation laws as proposed by Sellens (1987) and Li & Tankin (1988) do not give sufficient or proper information to predict realistic PDFs. We were unable to improve their results by postulating a meaningful extra constraint. Note that each constraint must have the specific form of [20], which all but facilitates the formulation of constraint if a complex process such as the break-up of a liquid sheet is studied.

However, it is not mandatory to put all physics in the form of constraints. Much relevant break-up process information is present in the Dombrowski & Johns (1963) model and is incorporated in the present model via the primary size distribution function. This approach must, of course, be accompanied by the invocation of a satellite distribution function. The latter has a clear physical meaning which renders the entire solution procedure powerful.

The two quasi-stationary states studied with the MEF are the ligament stage and the droplet flow, as depicted in figure 1. The evolution of one state into the other depends on the conservation laws and built-in physical constraints that have been formulated before. The MEF provides us with the PDF for the droplet flow that takes into account all these physical limitations and nothing else.

RESULTS AND DISCUSSION

Adjustable parameters and their relationships in the present model

The primary size distribution function, f_0, the satellite number density, $\tilde{N}$, and the dimensionless ligament diameter, $d_{\bar{lig}} \equiv d_{lig}/\delta_{30}$, are the main input parameters of the present model. The first function is described by the average value, $\langle \delta^* \rangle$, the variance, $1/(4k)$, and the amplitude A, see [7]. The function $\tilde{N}$ is described by three parameters b_i, see [12].

Several relations and restrictions hold for these parameters. Equation [11] links A to $d_{\bar{lig}}$; $\tilde{N}(d_{\bar{lig}})$ must be equal to 1; [13] links A to $\tilde{N}$. The accessible ranges of most parameters are well-confined, as shown above. In addition, all averages $\langle g_i \rangle$, or constants c, must be such that the system of governing equations can be solved properly and a realistic PDF obtained, see above and figure 6.

One way to take all the relations into account is by selecting merely two free parameters, $d_{\bar{lig}}$ and b_1. The amplitude A then follows from [11] and with some algebra it is easily shown that

$$b_2 = [1/A - 2 + b_1(d_{lig} + \langle \delta^* \rangle)]/(1/2k + \langle \delta^* \rangle^2 - d_{lig}^2),$$

from which b_0 follows according to $b_0 = 1 - b_1 d_{lig} - b_2 d_{lig}^2$.

Figure 9 is obtained with this procedure, and this typical result will be shown to be realistic. However, in our view, the parameter d_{lig} should be an experimentally-determined parameter, possibly dependent on, for example, nozzle type. The only experimental values of d_{lig} that are known to us have been obtained by Sellens (1987) (see [2]), and these are not particularly accurate data. The determination of the ligament thickness and the number of satellites for several nozzles under different conditions seems to be the next fundamental step in spray research. The connection of the ligament thickness with the number of satellites is given by [11] and it will be a real challenge to design an experiment in which the number of satellites, $1/A - 1$, is counted and δ_{30} and d_{lig} are measured simultaneously.

Until such experiments have been performed, the amplitude A can be considered as a parameter that must be close to the estimate given by [11] but is otherwise adjustable. Also the constraint on the averages, see figure 6, makes it more appropriate and convenient to loosen the ties between

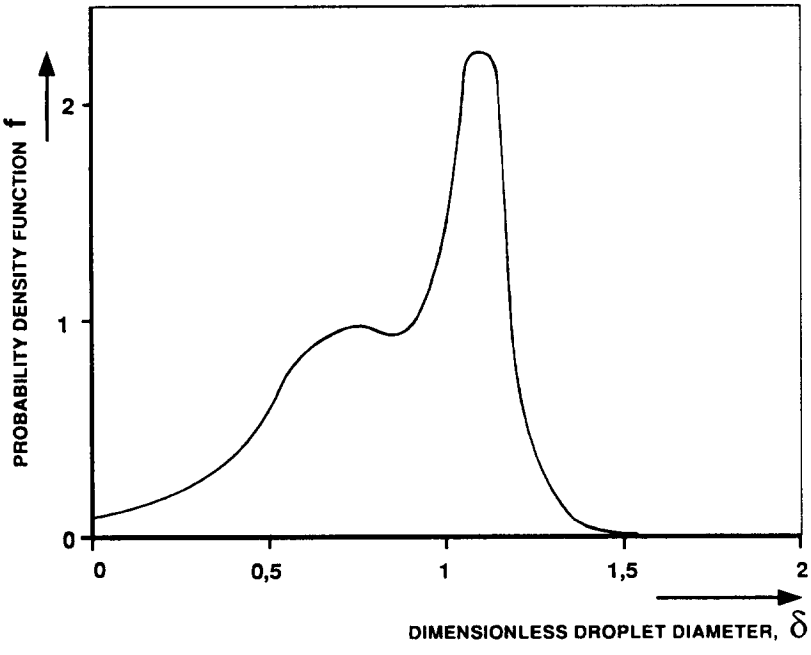

Figure 9. Example of a computed PDF: $\lambda_0 = 0.88272261$, $\lambda_1 = -6.2065696$, $\lambda_2 = 4.88484832$, $\lambda_3 = -20.38830255$, $\lambda_4 = 28.09509767$, $\lambda_5 = -126.69362377$, $\lambda_6 = 159.72616593$; $\tilde{N}(\delta^*) = 0.25372 + 0.93\delta^* + 0.14792\delta^{*2}$ if $\delta^* \geq 0.72$; $d_{lig} = 0.72$; $k = 70$; $A = 0.39684$; $\langle \delta^* \rangle = 1.15$.

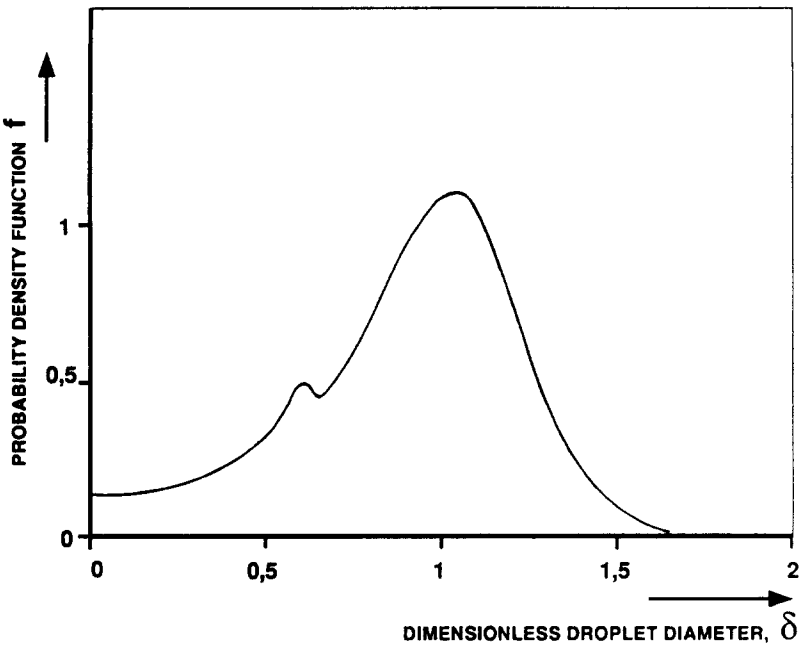

Figure 10. Example of a computed PDF: $\lambda_0 = 1.46592611$, $\lambda_1 = -1.74638951$, $\lambda_2 = 0.91995473$, $\lambda_3 = 2.51831839$, $\lambda_4 = -0.64876345$, $\lambda_5 = -5.76923076$, $\lambda_6 = 4.91309965$; $\tilde{N}(\delta^*) = 0.2256 + \delta^{*2}$ if $\delta^* \geqslant 0.88$; $d_{lig} = 0.88$; $k = 10$; $A = 0.384$; $\langle \delta^* \rangle = 1.15$.

A and d_{lig} and not to consider d_{lig} as the primary adjustment parameter. Figure 10 is obtained in this manner and it also shows a realistic PDF.

Our approach is phenomenological in the sense that there exist two parameters which must be adapted to the system parameters and upstream conditions. If we were to model quite different break-up processes, such as the break-up of cylindrical, turbulent jets, some parameters would have to be adapted. If, in addition, other physical mechanisms were involved, such as the transfer of kinetic energy between the turbulent air and the jet, additional constraints or parameters describing these mechanisms would have to be formulated. In any case, there is considerable potential for application to other modes of atomization. This makes it quite plausible that there are some parameters that must be adapted to the specific atomization mode. Apart from this, the natural freedom our model is rigorous and does not need arbitrary constants.

Trends and comparison with experiments

Figure 9 shows a typical predicted PDF. This PDF is fairly well balanced over all droplet diameters, implying that there is no surplus of small droplet sizes. It is noted that this result is achieved without invoking extra constraints or additional fit parameters, in contrast with the theoretical results of Sellens (1987).

Figures 9 and 10 also show that, as a consequence of satellite formation, the PDF shape, in general, becomes slightly bimodal. The extent to which this happens depends on the $\tilde{N}$ or the parameter b_1, which in principle could be measured independently. Such measurement would be extremely difficult and tedious, but so are direct and accurate measurements of PDFs. Sellens (1987) has measured PDFs quite close to the ligament stage to reduce the possiblity of size dispersion due to droplet interaction and interaction between droplets and the surrounding air. His PDFs all resemble those represented in figure 11. These PDFs are also bimodal, which is quite encouraging. Sellens (1987) describes the extra peak at a δ-value of about 0.5 as a "shoulder" and qualitatively explains its existence with radial entrainment effects affecting the localized measurements. In our view, the formation of satellites offers a much more natural explanation.

If the number of satellites is low with respect to the number of primary droplets, then the maximum of the computed PDF is largely determined by the maximum of the primary size PDF,

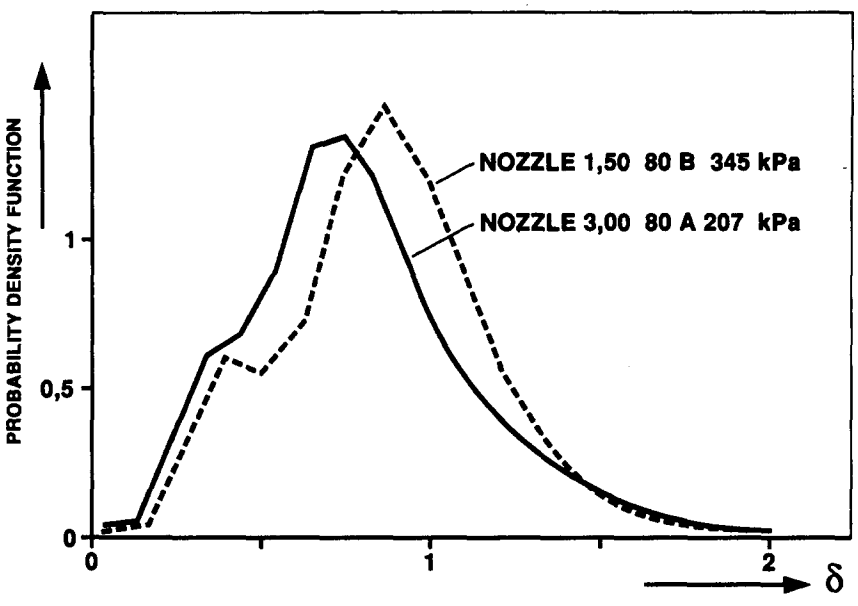

Figure 11. Typical examples of measured PDFs, after Sellens (1987).

f_0. This stands to reason, since satellite formation is then not the most dominant mechanism involved. The droplet diameter for which f_0 is maximum generally depends on the nozzle type and upstream conditions as discussed above.

How the predicted PDFs f and f_1 depend on the adjustable parameters is examined by varying one parameter at a time. The dependencies are now discussed and will be seen to stand to reason and to exhibit no sudden changes.

Increasing the value of b_1 or b_2 naturally increases the relative amount of small satellite. Increasing b_2 renders the PDF more pronouncedly bimodal than increasing b_1. Increasing the value of k naturally increases the maximum number of primary drops, since the spread in δ^* is proportional to $\sqrt{k}$, see figures 9 and 10.

Increasing d_{lig} or decreasing $\langle\delta^*\rangle$ increases the number of larger satellites relative to the number of small satellites and makes the PDF, f, look less bimodal. The effect of d_{lig} is trivial and is due to the fact that larger primary drops have more, although smaller, satellites due to growing liquid bridgings (see above and [3]). The effect of $\langle\delta^*\rangle$ is easily understood from the fact that the total mass of a unit cell is kept constant while varying $\langle\delta^*\rangle$.

Let the satellite distribution function, $f_1(\delta)$, have a maximum at δ_{max}. If δ^* increases, δ_{max} decreases and $f_1(\delta_{max})$ increases, as shown in figure 12. As argued before, larger primary drops have

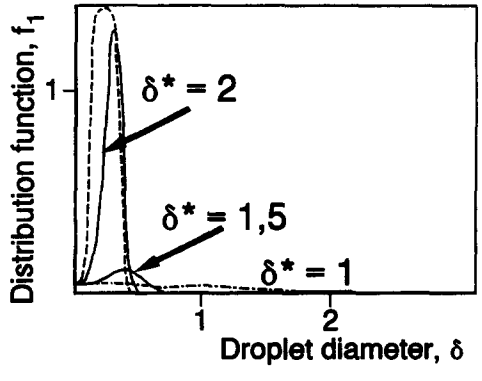

Figure 12. Specimens of the satellite distribution function, f_1, for some primary droplet sizes.

more, although smaller, satellites due to the increasing liquid bridgings, so this trend once again stands to reason. The computed satellite distribution functions satisfy approximately the normalization condition of [15a]. This result can be improved by increasing the number of moments of f_0 that are included in [16]. The rather high values of the Lagrange multipliers of the highest moments, λ_5 and λ_6, of figure 9 also show that increasing the number of moments in [16] would improve the results.

CONCLUSIONS

The MEF can be used to predict realistic size distributions. Apart from a standard normalization procedure the only physical constraints needed in the model are conservation of mass and conservation of surface energy. These constraints are applied to so-called unit cells only and not to the liquid sheet as a whole. The velocity PDF is seemingly inessential.

The predicted results are quite realistic, even for very small droplet sizes where other models failed without an artificial constraint.

Part of this success might be due to the fact that the model takes satellite formation into account. The primary droplet distribution function and the number of satellites are not known exactly *a priori* but are not critical and could, in principle, be determined with dedicated measurements.

Predicted PDFs have a tendency to be bimodal, which is in accordance with measurements performed relatively close to the liquid sheet (Sellens 1987). This correspondence indicates that satellite formation might be quite important. There exists some direct experimental validation of the satellite formation process in droplet clouds. However, the next fundamental step in spray research is the determination of ligament thickness, the number of satellites and the MMD simultaneously for several nozzles under different conditions.

Acknowledgements—The authors are grateful to Professor A. H. Lefebvre for his careful reading of the manuscript and to Dr R. W. Sellens for his useful comments.

REFERENCES

AGMON, N., ALHASSID, Y. & LEVINE, R. D. 1979 Algorithm for determining the Lagrange parameters in the maximum entropy formalism. In *The Maximum Entropy Formalism*, pp. 207–209. MIT Press, Cambridge, MA.

ALHASSID, Y., AGMON, N. & LEVINE, R. D. 1978 An upper bound for the entropy and its applications to the maximal entropy problem. *Chem. Phys. Lett.* **53,** 22–26.

BEER, J. M. & CHIGIER, N. A. 1972 *Combustion Aerodynamics*, pp. 154–155. Applied Science Publishers, New York.

BHATIA, J. C. & DURST, P. 1989 A comparative study of some probability distributions applied to liquid sprays. In *Proc. Int. Conf. on Mechanics of Two-phase Flows*, National Taiwan Univ., Taipei, pp. 279–284.

CHESTERS, A. K. 1990 Private communications. Eindhoven Univ. of Technology, The Netherlands.

DOMBROWSKI, N. & JOHNS, W. R. 1963 The aerodynamic instability and disintegration of viscous liquid sheets. *Chem. Engng Sci.* **18,** 203–214.

FRASER, R. P. & EISENKLAM, P. 1956 Liquid atomization and drop size of sprays. *Trans. Instn Chem. Engrs* **34,** 295–319.

VAN DER GELD, C. W. M. 1985 On phase distribution transitions in vertical evaporator tubes, pp. 215–260. Ph.D. Thesis, Eindhoven Univ. of Technology, The Netherlands.

VAN DER GELD, C. W. M. & NIJDAM, J. L. 1991 Bubble interaction and transition to plug flow. Presented at the *European Two-Phase Flow Gp Mtg*, Rome, Paper F1, pp. 6–17.

JAYNES, E. T. 1983 *Papers on Probability, Statistics and Statistical Physics*, pp. 60 & 210–315. Reidel, Dordrecht, The Netherlands.

LEFEBVRE, A. H. 1983 *Gas Turbine Combustion*, pp. 371–445. McGraw–Hill, New York.

LI, X. & TANKIN, R. S. 1988 Derivation of droplet size distribution in sprays by using information theory. *Combust. Sci. Technol.* **60,** 345–357.

MANSOUR, N. N. & LUNDGREN, T. S. 1990 Satellite formation in capillary jet breakup. *Phys. Fluids A* **2,** 1141–1144.

OHNESORGE, W. 1936 Die Bildung von Tropfen an Düsen und die Auflösung flüssiger Strahlen. *Z. Angew. Math. Mech.* **16,** 355–358.

RAYLEIGH, LORD 1878 On the instability of jets. *Proc. Lond. Math. Soc.* **10,** 4–13.

SELLENS, R. W. 1987 Drop size and velocity distributions in sprays. A new approach based on the maximum entropy formalism, pp. 6–18 & 71–78. Ph.D. Thesis, Univ. of Waterloo, Ontario.

SELLENS, R. W. & BRZUTOWSKI, T. A. 1986 A simplified prediction of droplet velocity distributions in a spray. *Combust. Flame* **65,** 273–279.

SHANNON, C. 1949 *The Mathematical Theory of Communication.* Univ. of Illinois Press, Urbana, IL.

TEBEL, K. H. 1982 Untersuchungen am zwangsgestörten Freistrahl, pp. 34–35. Ph.D. Thesis, Univ. of Cologne, Germany.

THEISSING, P. 1976 Erzeugung von flüssigkeitsfilmen, flüssigkeitslamellen und tropfen durch rotierende Scheiben. *VDI-Forsch.* **574,** 78–97.

WEBER, C. 1931 Zum zerfall eines flüssigkeitsstrahle. *Z. Angew. Math. Mech.* **11,** 136–159.

APPENDIX A

Derivation of f_1

Let $\mathbf{f}_1(\delta, \delta^*)\,\mathrm{d}\delta$ be the probability of finding precisely 1 satellite droplet with diameter in the range $[\delta, \delta + \mathrm{d}\delta)$ if a droplet with diameter δ^* is formed in a single unit. Let $\mathbf{f}_2(\delta, \delta^*)\,\mathrm{d}\delta$ be the probability of finding a total of precisely 2 satellite droplets with diameters in the range $[\delta, \delta + \mathrm{d}\delta)$ if a droplet with diameter δ^* is formed in a single unit. Similarly $\mathbf{f}_3$ etc. are defined (see figure 4). The probability of finding precisely 1 satellite droplet with diameter in the range $[\delta, \delta + \mathrm{d}\delta)$ is given by $\int f_0(\delta^*)\mathbf{f}_1(\delta, \delta^*)\,\mathrm{d}\delta^*$ etc. The probability of finding a droplet with diameter δ in the range $[\delta, \delta + \mathrm{d}\delta)$ in the droplet cloud after ligament break-up is now given by $f(\delta)\,\mathrm{d}\delta$, with

$$f(\delta) = f_0(\delta) + \int f_0(\delta^*)\mathbf{f}_1(\delta, \delta^*)\,\mathrm{d}\delta^* + 2\int f_0(\delta^*)\mathbf{f}_2(\delta, \delta^*)\,\mathrm{d}\delta^* + 3\int f_0(\delta^*)\mathbf{f}_3(\delta, \delta^*)\,\mathrm{d}\delta^* + \cdots.$$

The factor 2 in this equation stems from the fact that $\mathbf{f}_2$ is the probability for a pair of droplets, whereas f is the probability for a single bubble. Since it is not known *a priori* when the repeated break-up of liquid bridgings stops (see above), it is not clear where the series on the RHS of the above equation for f should end or how it converges. It is, therefore, condensed into

$$f(\delta) = f_0(\delta) + \int \tilde{N}(\delta^*) f_0(\delta^*) f_1(\delta, \delta^*)\,\mathrm{d}\delta^*.$$

The symbols used in this equation are defined and explained in the main text.

APPENDIX B

The Implementation of the MEF

The Lagrange multipliers are numerically determined with the aid of a Newton–Raphson procedure. Just as Stellens (1987) did, we enforced the normalization constraint at every iteration. For the numerical implementation, use was made of the algorithm of Alhassid *et al.* (1978) to promote convergence. Without this algorithm it is sometimes impossible to achieve convergence.

With one of the criteria of Alhassid *et al.* (1978), it is possible to examine whether the averages are properly balanced in the sense that realistic and sensible PDFs are produced. The impact of this balancing is illustrated in figure 6 for the sample case of two physical constraints:

$$\int f \, d\Omega = 1; \int f\delta^2 \, d\Omega = \langle g_1 \rangle; \int f\delta^3 \, d\Omega = \langle g_2 \rangle; f = \exp(-\lambda_0 - \lambda_1 \delta^2 - \lambda_2 \delta^3).$$

The lower border of the accessible region depicted in figure 6 follows from the criterion of Alhassid *et al.* (1978). Close to this border, the PDF is similar to Dirac's delta function. The upper border in the same figure follows from the demand that the PDF is integrable so must be bounded at infinity. If the averages are not well-balanced the latter demand is not fulfilled and computed PDFs are unrealistic, as exhibited by case C in figure 6. The higher the number of constraints that have to be fulfilled, the more difficult it is to find averages in the appropriate range.

It is noted that the integration accuracy may have a strong impact on the values of the Lagrangian multipliers. It may happen that convergence has seemingly been reached but that upon improving the integration accuracy the Lagrangian multipliers, and hence the PDF, drastically change. Before carrying out numerical integration all integrals are therefore reduced as much as possible to integrals of the type $\int t^q \cdot \exp[-k(t+\mu)^2] \, dt$, which are solved analytically. An adapted Romberg scheme is applied for the subsequent numerical integration.

APPENDIX C

Reduction of the Set of Governing Equations

In order to make [15a–c] more accessible, use is made of the primary size distribution function and the fact that f_0 is characterized by all its moments. Since the MEF can only determine multivariate single-valued functions, the product $f_0 \cdot f_1$ is redefined as $\hat{f}$. In principle, it is also allowable to solve for f_1 only, but this yields expressions of the type $\exp[\exp(q_1) \cdot q_2]$ with q_i a polynomial in δ and δ^* and these expressions are extremely difficult to integrate. In appendix B it is shown that the integration accuracy is very important in the MEF.

Equation [15a–c] is multiplied with $f_0(\delta^*) \cdot [\delta^* - \langle \delta^* \rangle]^s$, with s denoting the order of the moment of f_0, and is subsequently integrated over δ^*. Introducing $\tilde{f}$ and truncating after $s = 2$ yields the following set of integral equations:

$$\iint \tilde{f} \, d\delta \, d\delta^* = c_0^0, \quad \iint \delta^2 \tilde{N} \tilde{f} \, d\delta \, d\delta^* = c_1^0, \quad \iint \delta^3 \tilde{N} \tilde{f} \, d\delta \, d\delta^* = c_2^0; \qquad [C1]$$

$$\iint (\delta^* - \langle \delta \rangle^*) \tilde{f} \, d\delta \, d\delta^* = c_0^1, \quad \iint (\delta^* - \langle \delta \rangle^*) \delta^2 \tilde{N} \tilde{f} \, d\delta \, d\delta^* = c_1^1$$

$$\iint (\delta^* - \langle \delta \rangle^*) \delta^3 \tilde{N} \tilde{f} \, d\delta \, d\delta^* = c_2^1; \qquad [C2]$$

and

$$\iint (\delta^* - \langle \delta \rangle^*)^2 \tilde{f} \, d\delta \, d\delta^* = c_0^2, \quad \iint (\delta^* - \langle \delta \rangle^*)^2 \delta^2 \tilde{N} \tilde{f} \, d\delta \, d\delta^* = c_1^2,$$

$$\iint (\delta^* - \langle \delta \rangle^*)^2 \delta^3 \tilde{N} \tilde{f} \, d\delta \, d\delta^* = c_2^2; \qquad [C3]$$

with the constant $c_0^0 = A$ and the constant c_1^0 corresponding to the zero-order expansion and equal to the integral $\int (c_1 - \delta^{*2}) f_0(\delta^*) \, d\delta^*$, whose value is known. The other constants c_i^j are defined similarly. With the aid of the MEF [C1]–[C3] are solved to yield

$$\begin{aligned} \tilde{f} = \exp[&-\lambda_0 - \lambda_1 \delta^2 && -\lambda_2 \delta^3 + \\ &-\lambda_3(\delta^* - \langle \delta \rangle^*) - \lambda_4 \delta^2(\delta^* - \langle \delta \rangle^*) && -\lambda_5 \delta^3(\delta^* - \langle \delta \rangle^*) + \\ &-\lambda_6(\delta^* - \langle \delta \rangle^*)^2 - \lambda_7 \delta^2(\delta^* - \langle \delta \rangle^*)^2 && -\lambda_8 \delta^3(\delta^* - \langle \delta \rangle^*)^2 + \cdots]. \end{aligned} \qquad [C4]$$

APPENDIX D

Reduction of the Set of Lagrange Multipliers

In this appendix the proof is briefly outlined of the corollary stating that

$$\lambda_3, \lambda_9, \lambda_{15}, \ldots,$$

with each λ_i defined by [20], can be well-approximated by zero if k is sufficiently large. This corollary is useful in recognizing the distribution function $\tilde{f}$ as the product $f_0 f_1$.

For clarity and brevity, the following definitions are introduced: $y = \delta^* - \langle \delta^* \rangle$ and $g^+ = \int \tilde{f}\, d\delta$. Notice first that all constants, c, in [19] that are related to the Lagrangian multipliers in question are zero, due to the fact that f_0 is even, i.e. $c_0^1 = c_0^3 = c_0^5 = c_0^7 = \cdots = 0$. This implies that for each positive integer k,

$$0 = \int_{-\infty}^{\infty} y^k g^+(y)\, dy = \int_0^{\infty} y^k \{g^+(y) - g^+(-y)\}\, dy.$$

For each uneven function q, therefore,

$$\int_0^{\infty} q\{g^+(y) - g^+(-y)\}\, dy = 0.$$

In a similar manner it is shown that

$$\int_0^{\infty} v\{g^+(y) - g^+(-y)\}\, dy \approx 0$$

for each even function v. The approximation stems from the fact that the constant $\int y^{2p} f_0$ is inversely proportional to $2^{p+1} k^p \sqrt{k}$ and so it is not exactly zero in the lowest orders, although it rapidly approaches zero at higher order p. To a certain degree of approximation $[g^+(y) - g^+(-y)]$ is, therefore, equal to zero in the L^2-norm, implying that g^+ should be even. Since g^+ can be written as a product of $\exp(-\lambda_3 y - \lambda_9 y^3 - \cdots)$ and φ, with φ defined as $\int_{-\infty}^{\infty} s(\delta, y)\, d\delta$ for some function $s(\delta, y)$. Since φ is analytical at $y = 0$ it is not difficult to prove that only one function φ exists that satisfies the requirement that g^+ is even. However, φ contains independently variable Lagrangian multipliers so $\lambda_3 = \lambda_9 = \cdots = 0$.